Comparative Biochemistry and Physiology, Part C 230 (2020) 108699

Contents lists available at ScienceDirect

Comparative Biochemistry and Physiology, Part C

journal homepage: www.elsevier.com/locate/cbpc

Gill filament permeabilization: A novel approach to assess mitochondrial function in sheepshead minnows (*Cyprinodon variegatus*) following anthraquinone exposure

A. Reynolds Kirby[a], Gina Galli[b], Janna Crossley[a], Lauren E. Sweet[c], Dane A. Crossley II[a,*], Aaron P. Roberts[c]

[a] Developmental and Integrative Biology Division, Department of Biological Sciences, University of North Texas, Denton, TX, United States of America
[b] Faculty of Medical and Human Sciences, University of Manchester, Manchester, United Kingdom
[c] Advanced Environmental Research Institute, Department of Biological Sciences, University of North Texas, Denton, TX, United States of America

ARTICLE INFO

Keywords:
Oroboros Oxygraph
Mitochondrial respiration
ROS production
Proton leak
Photo-modified PAH
Gill filaments

ABSTRACT

Anthracene is a highly toxic polycyclic aromatic hydrocarbon (PAH), and its toxicity is increased 8-fold after compounding exposure to UV radiation. Exposure to either the parent or photo-modified compound has been shown to cause increases in reactive oxygen species (ROS) production and lipid peroxidation. Since the majority of ROS production occurs within mitochondria, we investigated simultaneous mitochondrial respiration and ROS production in the gills of sheepshead minnows (*Cyprinodon variegatus*) acutely (48 h) exposed to anthraquinone (40 μg l^{-1}). Anthraquinone exposure caused a 25% increase in oxidative phosphorylation with electrons donated to Complex I ($OXPHOS_{CI}$) and a 33% increase in Leak respiration with oligomycin ($Leak\text{-}Omy_{CI}$). ROS production was slightly increased (33.3%) in Leak state with oligomyocin respiring on Complex I substrates ($Leak\text{-}Omy_{CI}$) after anthraquinone exposure, but this value remained unchanged in all other respiratory states. When ROS production was normalized to mitochondrial oxygen consumption, we found that ROS production was decreased in all respiratory states, but most noticeably in the Leak state. We speculate that differences in the antioxidant defense system may have played a role in decreased ROS production. Overall, in this paper we present a novel technique to measure mitochondrial function in the gill filaments of teleost fish exposed to xenobiotic molecules, and we show anthraquinone exposure alters aspects of oxidative phosphorylation and ROS production.

1. Introduction

Polycyclic aromatic hydrocarbons (PAHs) are a carcinogenic compound found in smoke, tar, and crude oil. PAHs are released into the atmosphere by the burning and distilling of coal ore (Dipple, 1985), and into aquatic environments through the harvesting and transportation of crude oil (Pasparakis et al., 2019). Some PAHs contain photodynamic properties that are responsive to wavelengths in the UVA spectrum (315–400 nm) and can magnify toxicity in aquatic systems, resulting in photo-enhanced toxicity (Roberts et al., 2017). Photodynamic PAHs are excited by UVA light (380 nm), resulting in the formation of excited singlet and triplet state molecules. These molecules are highly reactive with their surrounding media and generate photo-modified PAHs (by-products), as well as reactive oxygen species (ROS), which enhances overall toxicity leading to oxidative stress (Arfsten et al., 1996; Mallakin et al., 1999). The photo-modified PAHs are typically oxidized, resulting in higher water solubility and bioavailability to aquatic organisms than the parent PAHs. These molecules are highly reactive in tissues and attach to membrane lipids, which compromise cellular and organelle membrane integrity (Sikkema et al., 1994).

Without the influence of UV, anthracene is a highly toxic PAH with an LC_{50} of approximately 16.6 μg $l^{-1,}$ which is enhanced eight-fold (LC_{50} of 1.94 μg l^{-1}) after co-UV exposure (Weinstein and Polk, 2001). Bluegill sunfish (*Lepomis macrochirus*) exposed to 12 μg l^{-1} of anthracene resulted in 100% mortality within nine hours of direct UV exposure (Bowling et al., 1983). The photo modification of anthracene (as a result of co-UV exposure) forms over 20 toxic byproducts (including anthraquinone), and generally the photoproducts are more toxic than the parent compounds (Mallakin et al., 1999). In the case of anthracene, 50% growth inhibition in aquatic duckweed (*Lemna gibba*) was achieved at a concentration of 1.0 mg l^{-1}, while the same growth inhibition was observed using photo-modified anthracene at lower

* Corresponding author.
E-mail address: dane.crossley@unt.edu (D.A. Crossley).

https://doi.org/10.1016/j.cbpc.2019.108699
Received 4 November 2019; Received in revised form 20 December 2019; Accepted 27 December 2019
Available online 31 December 2019

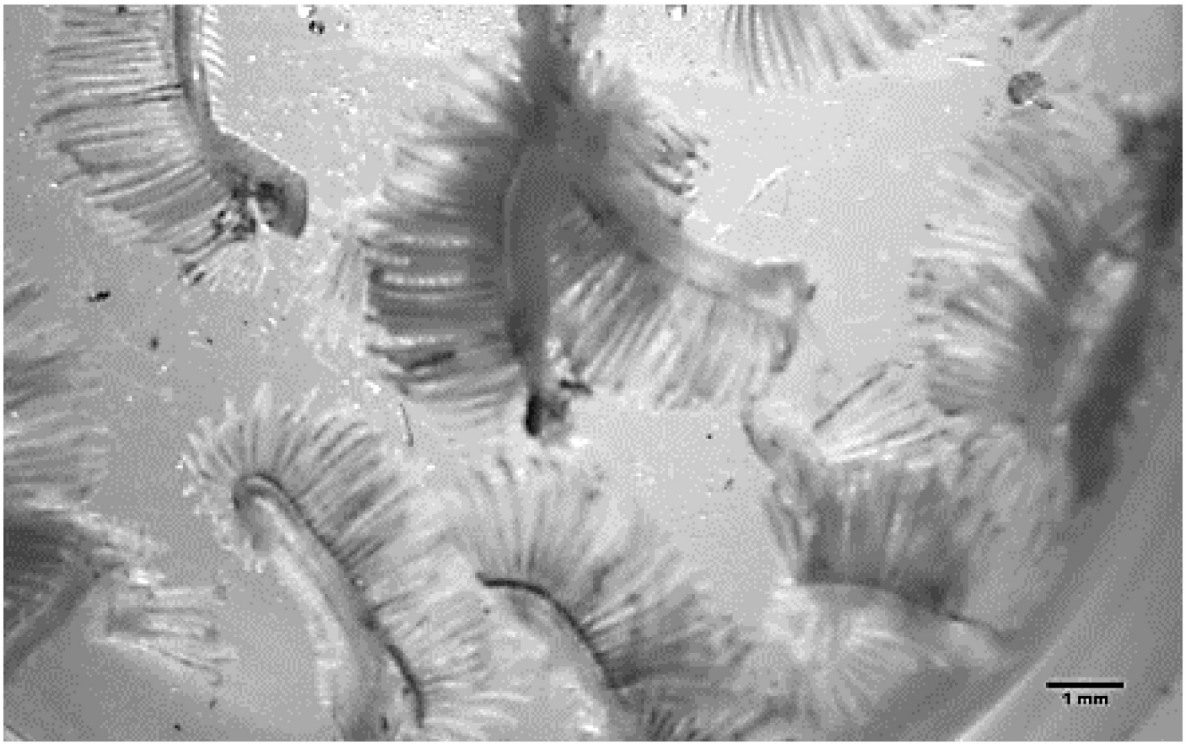

Fig. 1. Gill arches extracted from a Sheepshead Minnow (*Cyprinodon variegatus*) and viewed under a Lecia EZ4 dissecting scope prior to permeabilization.

concentrations (0.1 mg l^{-1}) (Huang et al., 1995). Photodynamic PAHs (anthracene) absorb UV radiation resulting in an excited energy state and oxidized photoproducts (anthraquinone). The energy released as the excited compound returns to the ground state and can be transferred directly to cellular O_2 or membrane lipids (Roberts et al., 2017). This process of photosensitization has been proposed as the mechanism of toxicity (for PAHs and their photoproducts) through the production of reactive oxygen species (ROS), resulting in oxidative damage to tissues and membranes (Mallakin et al., 1999; Roberts et al., 2017; Weinstein and Polk, 2001). In fact, markers of oxidative stress (increased lipid peroxidation and ROS production) were found in bluegill sunfish liver microsomes after 60 min of exposure to anthracene (3.015 μg ml^{-1}) and UV light (Choi and Oris, 2000).

Considering that ROS production occurs in the mitochondrial complexes, we wanted to measure the effects of anthraquinone on mitochondrial function (oxygen consumption and coupling efficiency) while simultaneously measuring ROS production in sheepshead minnow (*Cyprinodon variegatus)* gill filaments. We chose the gill filament as a target tissue because PAHs easily flux across the gill epithelium and are rapidly dispersed into the bloodstream (Ramachandran et al., 2006). In the past, oxidative phosphorylation of the gills has been measured in purified isolated mitochondria. However, this preparation requires large tissue samples, which is not possible in small fish species, such as the sheepshead minnow. To this end, we have developed a novel, whole permeabilized gill filament preparation to assess mitochondrial function and simultaneous ROS production in sheepshead minnows following acute (48 h) anthraquinone exposure. Permeabilization of the tissue removes the influence of the antioxidant defense systems and cascade signaling and gives us access to the electron transport chain for pharmacological manipulations (Pesta and Gnaiger, 2012). Here we show that the permeabilized gill preparation is suitable for mitochondrial measurements and can be successfully utilized for toxicological investigations.

2. Materials and methods

2.1. Animals

Adult, mix-sexed Sheepshead Minnows (*Cyprinodon variegatus*) were purchased from Aquatic Biosystems (Fort Collins, CO) and overnighted to the University of North Texas. Upon arrival, minnows were housed in 100 l tanks filled with 25 ppt saltwater maintained at 26 °C. Saltwater was mixed in the lab by combining deionized facility water with Instant Ocean® Sea Salt (United Pet Group, Blacksburg, VA). Minnows were kept on a 10:14 h light:dark photoperiod and fed pellet food (Skretting, Tooele, UT) *ad libitum* every other day, except 24 h prior to experimentation. Water quality (pH [6.8–7.5], ammonia [< 5 ppm], nitrite [< 1.0 ppm], nitrate [< 40 ppm]) parameters were monitored daily.

2.2. Acute (48 h) anthraquinone exposure

Adult minnows (two per replicate) were moved to 20 l exposure tanks filled with 25 ppt saltwater maintained at 26 °C. One tank contained anthraquinone (40 μg l^{-1}) dissolved in dimethyl sulfoxide (DMSO), and the other tank contained an equal volume of DMSO to serve as a vehicle control. After 24 h, minnows were transferred to new aquaria that were filled with 25 ppt saltwater and a dose of either anthraquinone (40 μg l^{-1}) or DMSO (equal volume). A 48 h static renewal exposure is a fairly standard procedure when assessing compound toxicity and is used as a precaution of biodegradation and volatilization (Weinstein and Polk, 2001). The concentration of anthraquinone used in this study is within environmentally relevant levels (less than 10 μg l^{-1}) for anthracene and related byproducts. Temperature and oxygen saturation were monitored throughout experimentation using a handheld YSI dissolved oxygen probe (YSI, Inc., Yellow Springs, OH). Water parameters (pH, ammonia, nitrate, and nitrate) were monitored throughout the exposure period. After 48 h, the trial was terminated and minnows were euthanized using a lethal dose of buffered MS-222 (100 mg l^{-1} MS-222 and 200 mg l^{-1} $NaHCO_3$). Gill baskets were removed from both sides of the fish and immediately

processed according to the procedures below.

2.3. Permeabilized gill filament preparation

Gill arches were placed in ice-cold BIOPS (pH 7.1) containing [2.8 mM CaK_2EGTA (pH 7.0), 7.2 mM K_2EGTA (pH 7.0), 5.8 mM Na_2ATP, 6.6 mM $MgCl_2{\cdot}6H_2O$, 20 mM Taurine, 15 mM Na_2 Phosphocreatine, 20 mM Imidazole, 0.5 mM Dithiothreitol, and 50 mM 2-(N-morpholino) ethanesulfonic acid] (Galli et al., 2016). Under a Lecia EZ4 dissecting scope (Lecia Microsystems Inc., Buffalo Grove, IL) with a dark background, mucous and blood clots were removed from the gill arches (Fig. 1). Gill arches were incubated at 4 °C in BIOPS with saponin (50 μg ml^{-1}) on an orbital shaker (Cole-Parmer, Vernon Hills, IL) for 12 min at speed two. Arches were triple washed (to remove excess lipids) for 10 min in 4 °C MIR05 respiration medium (pH 7.1) containing [0.5 mM EGTA, 3.0 mM $MgCl_2{\cdot}6H_2O$, 60 mM K-2-(N-morpholino) ethanesulfonic acid, 20 mM Taurine, 10 mM KH_2PO_4, 20 mM HEPES, 110 mM D-Sucrose, 1% BSA] (Galli et al., 2016). Gill filaments were cut from the arches and wet weight was recorded. Gill filaments (wet weight 2 mg) were added to each chamber of an Oroboros Oxygraph 2 K HR respirometer (Oroboros Instruments, Innsbruck, Austria) containing MIR05 respiration solution maintained at 30 °C. The chambers were hyper-oxygenated and oxygen concentration was maintained between 200 and 400 nm ml^{-1} during each trial. Mitochondrial function analyses were conducted in two parts: 1) measurement of mitochondrial respiration with simultaneous ROS production and 2) a cytochrome *c* test with measurement of $OXPHOS_{CIV}$. This was done because cytochrome *c* and TMPD with ascorbate (complex IV substrates) are strong redox substances that consume H_2O_2 which interferes with the H_2O_2 calibration and overall sensitivity of the method (Makrecka-Kuka et al., 2015).

The Oroboros was outfitted with O2K-fluorescence LED probes (Oroboros Instruments, Innsbruck, Austria) to detect ROS flux within the Oxygraph chambers. The following protocol measuring simultaneous ROS production and mitochondrial respiration is modified from previously published studies (Krumschnabel et al., 2015; Suski et al., 2012). Amplex™ UltraRed (10 μM), horseradish peroxidase (1 U/ml), and superoxide dismutase (10 U/ml) were injected into each chamber to induce oxidation of Amplex™ UltraRed to red-fluorescent resorufin in the presence of H_2O_2. The fluorescent signal was calibrated by stepwise injections of 400 μM H_2O_2 (final concentration; 0–2 mM).

2.4. Protocol 1: respiratory states and ROS production

Respiratory substrates malate (2 mM) and pyruvate (5 mM) were injected into the chambers and served as a measurement for LEAK respiration without adenylates while respiring on Complex I substrates ($LEAK\text{-}LN_{CI}$; Table 1). Succinate (10 mM) was added to the chamber to measure LEAK respiration with Complex I and II substrates without adenylates ($LEAK\text{-}LN_{CI+CII}$; Table 1). $OXPHOS_{CI+CII}$ (Table 1) was induced by adding saturating levels of ADP (5 mM). Oligomycin (2 μg ml^{-1}) was then added to the chambers to block the ATP synthase and measure LEAK state with Oligomycin ($LEAK\text{-}Omy_{CI+CII;}$ Table 1). Rotenone (0.5 μM) was titrated into the chambers to inhibit Complex I of the ETS and measure $LEAK\text{-}Omy_{CII}$ (Table 1). Lastly, Antimycin A (2.5 μM) was added to the chambers to measure residual oxygen consumption (ROX) or chamber respiration not attributed to mitochondrial respiration (Table 1).

2.5. Protocol II: cytochrome C test and $OXPHOSC_{IV}$ respiration

Malate (2 mM), and pyruvate (5 mM) were added to provide carriers for the citric acid cycle. Saturating concentrations of ADP (5 mM) were injected into the chambers to initiate $OXPHOS_{CI,}$ and succinate (10 mM) was added to provide substrates for complex II activation ($OXPHOS_{CI+CII}$; Table 1). Cytochrome c (10 μM) was added to assess mitochondrial quality and to determine inner mitochondrial membrane integrity after permeabilized gill filament preparation (Table 1). $OXPHOS_{CIV}$ was stimulated through tetramethyl-*p*-phenylene-diamine (TMPD; 0.5 mM) and ascorbate (2 mM) injections (Table 1).

2.6. Calculations and statistical analysis

Trials were excluded from the data analysis when respiration rate increased above 15% after cytochrome *c* injection and when respiratory control ratios (RCR) were lower than 6, which indicated a damaged preparation (Brand and Nicholls, 2011). All fluxes were corrected for background O_2 consumption by subtracting the respiration rate after gills were added but before mitochondrial substrates and inhibitors were added. Respiration rate and ROS production were normalized to the wet weight of the gill filaments and expressed as pmol sec^{-1} mg wet wt^{-1}. The respiratory control ratio (RCR) was calculated by dividing $OXPHOS_{CI+CII}$ respiration rate by $LEAK_{LNCI+CII}$ in protocol I. All statistical tests were performed using Statistica Version 13.3. A repeated-measures ANOVA with a Tukey HSD test was used to make comparisons in mitochondrial respiration and ROS production between treatments. A student's *t*-test was used to check for difference at $OXPHOS_{CIV}$ and RCRs between control and exposed minnows.

3. Results and discussion

To date, the effects of individual PAH exposure on intact mitochondrial function are relatively unknown. Few studies have highlighted the effects of crude oil exposure on mitochondrial function, which provided the framework for our investigation. We have developed a new preparation for measuring mitochondrial function in whole gill preparations from small fish. Furthermore, we have shown exposure to anthraquinone affects aspects of mitochondrial electron transport chain function and ROS production.

3.1. Development of a permeabilized whole-gill mitochondrial preparation

Permeabilized mitochondrial preparations allow detailed characterization of electron transport chain function in their normal intracellular position, thus preserving essential interactions with the cytoskeleton and other organelles. We adapted protocols for skeletal muscle preparations to develop a permeabilized whole-gill preparation (Fig. 1). Our RCR values (control: 3.88 ± 0.49 and exposed: 4.42 ± 0.42) from permeabilized gill filaments are consistent with published values in teleost cardiac and skeletal muscle (Fig. 2A; Chung et al., 2017; Guderley and Johnston, 1996; Iftikar and Hickey, 2013). Furthermore, there were negligible effects of Cytochrome C, which suggests the inner mitochondrial membrane was intact. Taken together, these results suggest the fibers were of excellent quality with no overt signs of dysfunction from the permeabilization process (Brand and Nicholls, 2011). Therefore, we consider this preparation is appropriate for studying mitochondrial function in whole-gills, which is particularly useful for studies in small fish.

3.2. Effects of anthraquinone on electron transport chain function and ROS production

There was a tendency for anthraquinone exposure to cause an increase in oxygen consumption across all respiratory states. This effect was particularly pronounced, and statistically significant, when Complex I and II substrates were combined in both the OXPHOS and Leak-Omy states (Fig. 2A, B). The fact that both Leak and OXPHOS increased with anthraquinone exposure meant that RCR's ratios were similar between exposed minnows and controls (3.88 ± 0.49 and 4.42 ± 0.44 respectively), suggesting that mitochondrial efficiency remained unchanged. These results suggest anthraquinone exposure increases mitochondrial oxidative capacity in minnows. Given that ATP

Table 1
The action and subsequent mitochondrial states as a result of substrates and inhibitors used in Protocol I and II.

	Action	State	Electron entry	Abbreviation
Protocol I				
Malate (2 mM) pyruvate (5 mM)	Citric acid cycle and glycolysis intermediates. Substrates for Complex I-linked respiration	Leak respiration without adenylates (LN)	Complex I	Leak-LN_{CI}
Succinate (10 mM)	Citric acid cycle intermediate. Substrate for Complex II-linked respiration	Leak respiration without adenylates (LN)	Complex I & II (convergent electron entries into the Q-junction)	Leak-LN_{CI+CII}
Saturating ADP (5 mM)	Substrate for ATP synthase	OXPHOS respiration	Complex I & II	$OXPHOS_{CI}$
Oligomycin (2 μg ml^{-1})	Inhibitor of the $F_1F_oATPase$ (Complex V)	Leak state induced with oligomycin	Complex I & II	Leak-Omy_{CI+CII}
Rotenone (0.5 μM)	Inhibitor of Complex I	Leak state induced with oligomycin	Complex II	Leak-Omy_{CII}
Antimycin A (2.5 μM)	Inhibitor of Complex III	Residual oxygen consumption	N/A	ROX
Respiratory Control Ratio	Indicates the degree of coupling OXHPOS and ATP synthase	$OXPHOS_{CI-CIV}$/Leak-LN_{CI+CII}	N/A	RCR
Protocol II				
Malate (2 mM) pyruvate (5 mM)	Citric acid cycle and glycolysis intermediates, respectively. Substrates for Complex I-linked respiration	Leak respiration without adenylates (LN)	Complex I	Leak-LN_{CI}
ADP (5 mM)	Substrate for ATP synthase	OXPHOS respiration	Complex I & II	$OXPHOS_{CI}$
Succinate (10 mM)	Citric acid cycle intermediate. Substrate for Complex II-linked respiration	Leak respiration without adenylates (LN)	Complex I & II	$OXPHOS_{CI+CII}$
Cytochrome C (10 μM)	Component of the electron transport chain	N/A	N/A	N/A
Ascorbate (2 mM)	Antioxidant to prevent autoxidation of TMPD (see next step)	N/A	N/A	N/A
Tetramethyl-*p*-phenylene-diamine (TMPD; 0.5 mM)	Electron donor to Complex IV	OXPHOS respiration	Complex IV	$OXPHOS_{CIV}$

demand is increased during toxic exposure (e.g., recruitment of ATP-dependent ion channels), a greater mitochondrial capacity may represent a compensatory mechanism to match ATP supply to demand during environmental stress.

Anthraquinone exposure led to a 30% increase in ROS production during Leak-Omy_{CI+CII} respiratory state (Fig. 2C). However, a different pattern emerged when ROS production was normalized to mitochondrial oxygen consumption. For all leak respiratory states (Leak-Ln_{CI}, Leak-Omy_{CI+CII}, Leak-Omy_{CII}), ROS production was reduced by 20 to 40% in mitochondria from minnows exposed to anthraquinone (Fig. 2D). Therefore, after differences in oxygen consumption are taken into account, our results suggest ROS production is lower in minnows exposed to anthraquinone, compared to controls. While we did not address the mechanism underlying the differences in ROS production, it is possible that minnows exposed to anthraquinone may mount a protective response by actively suppressing pathways involved in ROS production, or upregulating the antioxidant defense system (Regoli et al., 2011). Support for the latter hypothesis comes from studies in liver mitochondria of goldfish (*Carassius auratus*), which showed levels of superoxide dismutase and catalase were elevated in exposed to phenanthrene exposure (a PAH that is abundant in aquatic systems) (Yin et al., 2007). Nevertheless, it is possible that the exposure length or

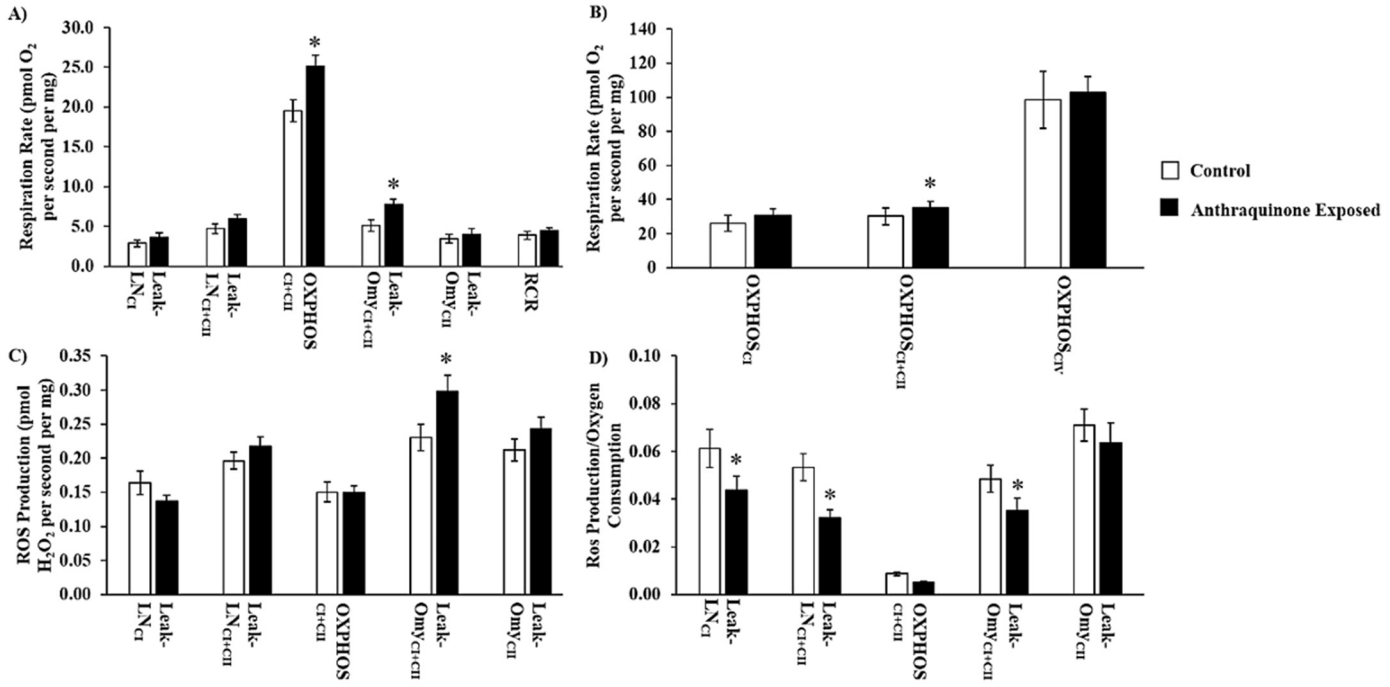

Fig. 2. Protocol one measurements of mitochondrial respiration (A) and simultaneous ROS production (C) after 48 h of exposure in control tanks (open bars) or in anthraquinone (40 μg l^{-1}) dosed tanks (closed bars). Measurements from protocol two on OXPHOS respiration (B). ROS production normalized for mitochondrial respiration rate (D). Data are represented as means ± s.e. Single asterisk denotes significant differences between treatments ($p < 0.05$).

concentration was not long or high enough to overwhelmed the antioxidant defense system, leading to an increase in ROS production, similar to previous studies (Yin et al., 2007). Further research is necessary to resolve these speculations, which could include measurements of antioxidants and markers of oxidative damage (lipid peroxidation).

In contrast to our study, Xu et al. (2017) found that larval red drum (*Sciaenops ocellatus*) exposed to crude oil concentrations of 4.8 μg l^{-1} ΣPAH_{50} at 24,h, 48 h, and 72 h had differential transcription profiles that were consistent with changes in mitochondrial function, mitochondrial transmembrane potential, oxidative stress response pathways, and cell death signaling (Xu et al., 2017). In adult red drum, mitochondrial function and performance was assessed following 24 h exposure at concentrations of 29.6 ± 7.4 μg l^{-1} and 64.5 ± 8.9 μg l^{-1} ΣPAH_{50} and they found no change in Leak respiration, maximal ETS, or coupling controls ratios (markers of mitochondrial dysfunction) after 24 h of crude oil exposure (Johansen and Esbaugh, 2019). Mitochondrial function has also been measured in adult Mahi-mahi (*Coryphaena hippurus*) that were exposed to crude oil (9.6 ± 1.7 μg l^{-1} ΣPAH_{50}) for 24 h and the authors determined that while $OXPHOS_{CI}$ and $OXPHOS_{CII}$ respiration was decreased, classic markers of mitochondrial dysfunction were not observed (no change in leak respiration, maximal ETS, or coupling control ratios) (Kirby et al., 2019). It should be mentioned that the crude oil concentrations used in the 24 h exposures are environmentally relevant to concentrations that occurred during the Deepwater Horizon Oil Spill (Wade et al., 2011) and the lowest doses were previously shown to affect swim performance and aerobic scope in adult fish (Johansen and Esbaugh, 2017; Mager et al., 2014). Taken together, these studies and ours suggest the effects of crude oil and their constituents on fish mitochondrial function are variable and unpredictable. Clearly, more research needs to be conducted in other areas of mitochondrial bioenergetics to determine the mechanisms of toxicity that crude oil and individual PAH have on teleost mitochondrial function.

Declaration of competing interest

No conflicts of interest, financial or otherwise, are declared by the author(s).

Acknowledgments

This research was made possible by a grant from The Gulf of Mexico Research Initiative. Data are publicly available through the Gulf of Mexico Research Initiative Information & Data Cooperative (GRIIDC) at https://data.gulfresearchinitiative.org (doi: https://doi.org/10.7266/N71Z4304).

References

Arfsten, D.P., Schaeffer, D.J., Mulveny, D.C., 1996. The effects of near ultraviolet radiation on the toxic effects of polycyclic aromatic hydrocarbons in animals and plants: a review. Ecotoxicol. Environ. Saf. 33 (1), 1–24. https://doi.org/10.1006/eesa.1996.0001.

Bowling, J., Leversee, G., Landrum, P., Giesy, J., 1983. Acute mortality of anthracene-contaminated fish exposed to sunlight. Aquat. Toxicol. 3 (1), 79–90.

Brand, M.D., Nicholls, D.G., 2011. Assessing mitochondrial dysfunction in cells. Biochem. J. 435 (Pt 2), 297–312. https://doi.org/10.1042/BJ20110162.

Choi, J., Oris, J.T., 2000. Evidence of oxidative stress in bluegill sunfish (Lepomis macrochirus) liver microsomes simultaneously exposed to solar ultraviolet radiation and anthracene. Environ. Toxicol. Chem. 19 (7), 1795–1799. https://doi.org/10.1002/etc.5620190713.

Chung, D.J., Bryant, H.J., Schulte, P.M., 2017. Thermal acclimation and subspecies-specific effects on heart and brain mitochondrial performance in a eurythermal teleost (< em > Fundulus heteroclitus < /em >). J. Exp. Biol. 220, 1459–1471.

Dipple, A., 1985. Polycyclic Aromatic Hydrocarbon Carcinogenesis. 283. pp. 1–17. https://doi.org/10.1021/bk-1985-0283.ch001.

Galli, G.L.J., Crossley, J., Elsey, R.M., Dzialowski, E.M., Shiels, H.A., Crossley, D.A., 2016. Developmental plasticity of mitochondrial function in American alligators, < em > Alligator mississippiensis < /em > Am. J. Physiol. Regul. Integr. Comp. Physiol. 311, R1164–R1172.

Guderley, H., Johnston, I., 1996. Plasticity of fish muscle mitochondria with thermal acclimation. J. Exp. Biol. 199, 1311–1317.

Huang, X.D., Dixon, D.G., Greenberg, B.M., 1995. Increased polycyclic aromatic hydrocarbon toxicity following their photomodification in natural sunlight: impacts on the duckweed Lemna gibba L. G-3. Ecotoxicol. Environ. Saf. 32, 194–200.

Iftikar, F.I., Hickey, A.J.R., 2013. Do mitochondria limit hot fish hearts? Understanding the role of mitochondrial function with heat stress in Notolabrus celidotus. PLoS One 8, e64120.

Johansen, J.L., Esbaugh, A.J., 2017. Sustained impairment of respiratory function and swim performance following acute oil exposure in a coastal marine fish. Aquat. Toxicol. 187, 82–89.

Johansen, J.L., Esbaugh, A.J., 2019. Oil-induced responses of cardiac and red muscle mitochondria in red drum (Sciaenops ocellatus). Comparative Biochemistry and Physiology Part C: Toxicology & Pharmacology 219, 35–41.

Kirby, A.R., Cox, G.K., Nelson, D., Heuer, R.M., Stieglitz, J.D., Benetti, D.D., Grosell, M., Crossley, D.A., 2019. Acute crude oil exposure alters mitochondrial function and ADP affinity in cardiac muscle fibers of young adult Mahi-mahi (Coryphaena hippurus). Comparative Biochemistry and Physiology Part C: Toxicology & Pharmacology 218, 88–95.

Krumschnabel, G., Fontana-Ayoub, M., Sumbalova, Z., Heidler, J., Gauper, K., Fasching, M., Gnaiger, E., 2015. Simultaneous high-resolution measurement of mitochondrial respiration and hydrogen peroxide production. Methods Mol. Biol. 1264, 245–261. https://doi.org/10.1007/978-1-4939-2257-4_22.

Mager, E.M., Esbaugh, A.J., Stieglitz, J.D., Hoenig, R., Bodinier, C., Incardona, J.P., Scholz, N.L., Benetti, D.D., Grosell, M., 2014. Acute embryonic or juvenile exposure to Deepwater horizon crude oil impairs the swimming performance of mahi-mahi (Coryphaena hippurus). Environ Sci Technol 48, 7053–7061.

Makrecka-Kuka, M., Krumschnabel, G., Gnaiger, E., 2015. High-resolution respirometry for simultaneous measurement of oxygen and hydrogen peroxide fluxes in permeabilized cells, tissue homogenate and isolated mitochondria. Biomolecules 5 (3), 1319–1338. https://doi.org/10.3390/biom5031319.

Mallakin, A., McConkey, B.J., Miao, G., McKibben, B., Snieckus, V., Dixon, D.G., Greenberg, B.M., 1999. Impacts of structural photomodification on the toxicity of environmental contaminants: anthracene photooxidation products. Ecotoxicol. Environ. Saf. 43, 204–212.

Pasparakis, C., Esbaugh, A.J., Burggren, W., Grosell, M., 2019. Impacts of Deepwater horizon oil on fish. Comparative Biochemistry and Physiology Part C: Toxicology & Pharmacology 224, 108558. https://doi.org/10.1016/j.cbpc.2019.06.002.

Pesta, D., Gnaiger, E., 2012. High-resolution respirometry: OXPHOS protocols for human cells and permeabilized fibers from small biopsies of human muscle # *T Mitochondrial*. Bioenergetics 810, 25–58.

Ramachandran, S.D., Sweezey, M.J., Hodson, P.V., Boudreau, M., Courtenay, S.C., Lee, K., King, T., Dixon, J.A., 2006. Influence of salinity and fish species on PAH uptake from dispersed crude oil. Mar. Pollut. Bull. 52, 1182–1189.

Regoli, F., Giuliani, M.E., Benedetti, M., Arukwe, A., 2011. Molecular and biochemical biomarkers in environmental monitoring: a comparison of biotransformation and antioxidant defense systems in multiple tissues. Aquat. Toxicol. 105, 56–66.

Roberts, A.P., Alloy, M.M., Oris, J.T., 2017. Review of the photo-induced toxicity of environmental contaminants. Comparative Biochemistry and Physiology Part C: Toxicology & Pharmacology 191, 160–167.

Sikkema, J., de Bont, J.A., Poolman, B., 1994. Interactions of cyclic hydrocarbons with biological membranes. J. Biol. Chem. 269 (11), 8022–8028.

Suski, J.M., Lebiedzinska, M., Bonora, M., Pinton, P., Duszynski, J., Wieckowski, M.R., 2012. Relation between mitochondrial membrane potential and ROS formation. Methods Mol. Biol. 810, 183–205. https://doi.org/10.1007/978-1-61779-382-0_12.

Wade, T.L., Sweet, S.T., Sericano, J.L., Guinasso, N.L., Diercks, A.R.R., Highsmith, R.C., Asper, V.L., Joung, D.D., Shiller, A.M., Lohrenz, S.E., 2011. Analyses of water samples from the Deepwater horizon oil spill: documentation of the subsurface plume. Monitoring and Modeling the deepwater horizon oil spill: a record-breaking enterprise 77–82.

Weinstein, J.E., Polk, K.D., 2001. Phototoxicity of anthracene and pyrene to glochidia of the freshwater mussel Utterbackia imbecillis. Environ. Toxicol. Chem. 20, 2021–2028.

Xu, E.G., Khursigara, A.J., Magnuson, J., Hazard, E.S., Hardiman, G., Esbaugh, A.J., Roberts, A.P., Schlenk, D., 2017. Larval red drum (Sciaenops ocellatus) sublethal exposure to weathered Deepwater horizon crude oil: developmental and transcriptomic consequences. Environmental Science & Technology 51, 10162–10172.

Yin, Y., Jia, H., Sun, Y., Yu, H., Wang, X., Wu, J., Xue, Y., 2007. Bioaccumulation and ROS generation in liver of Carassius auratus, exposed to phenanthrene. Comparative Biochemistry and Physiology Part C: Toxicology & Pharmacology 145, 288–293.